PHYSICAL REVIEW D **95,** 113001 (2017)

Decay constants and distribution amplitudes of B meson in the relativistic potential model

Hao-Kai Sun* and Mao-Zhi Yang†

School of Physics, Nankai University, Tianjin 300071, People's Republic of China

(Received 6 October 2016; published 6 June 2017)

In this work we study the decay constants of B and B_s mesons based on the wave function obtained in the relativistic potential model. Our results are in good agreement with experimental data which enables us to apply this method to the investigation of B-meson distribution amplitudes. A very compact form of the distribution amplitude is obtained. We also investigate the one-loop QCD corrections to the pure leptonic decays of B mesons. We find that, after subtracting the infrared divergence in the one-loop corrections using the factorization method, the QCD one-loop corrections to the hard amplitude of leptonic decay will be zero.

DOI: 10.1103/PhysRevD.95.113001

I. INTRODUCTION

The study of B-meson decays, especially the exclusive semileptonic and two-body nonleptonic decays, presents rich information for testing and understanding the standard model (SM). In the past two decades, as the running and upgrading of B-factories, a great amount of experimental data has been accumulated. Although a lot of models and/or approaches have been developed in theory, the poor knowledge of nonperturbative quantum chromodynamics (QCD) effects still limits theoretical predictions severely. In two-body nonleptonic decays of B-meson, QCD factorization [1–4] and perturbative QCD approaches [5–9] have been developed, which allow us to separate the nonperturbative effect out as universal quantities, such as, the light-cone distribution amplitudes (LCDA) and/or form factors. The B-meson LCDA has been studied extensively. Several forms of the distribution amplitudes are proposed or obtained by some theoretical methods such as solving the equations of motion in the literature [10–18].

Inspired by the construction of initial bound state in Ref. [19] and based on our previous works on the mass spectrum and wave functions of B-meson [20–22], we try an alternate way to study the distribution amplitudes with the help of wave functions obtained in the relativistic potential model [21,22]. Considering the recent experimental data on the pure leptonic decays of B mesons, we focus on a careful investigation about the decay constants and the distribution amplitudes (DAs) of B-mesons in this paper.

In general, the decay constants of charged heavy-light mesons are related directly to the pure leptonic decay widths and thus measuring decay constants can provide a chance to check different theoretical models and may also give some hints for physics beyond the standard model (SM). During the past decades, many methods have been applied to the study of the decay constants, such as, QCD sum rules [23–29], the Bethe-Salpeter equation [30,31], the field correlator method [32], the soft-wall holographic approach [33], the potential models [20,34–37], and the lattice QCD simulations [38–45], etc. Up to now there are still large uncertainties for the value of $|V_{ub}|$ [46], and only the pure leptonic decay mode of B meson with τ lepton in the final state has been measured in experiment [47–50] (also with large uncertainties). Our result for the branching ratio of $B \to \tau\nu$ decay is well located in the experimental error bars [47–51]. Further tests from experiments are needed in the future with enhanced precision (most possibly come from the Belle II/SuperKEKB collaboration [52,53]).

We study the B-meson distribution amplitudes in this work. The analytical forms both in coordinate and momentum space are obtained. When they are transformed to the commonly used form of LCDA, the figures show that they obey the model-independent limitations [13]. We also consider the pure leptonic decays of B-meson up to one-loop level in QCD corrections. We find that one-loop corrections to the hard-scattering kernel in QCD will be zero after subtracting the infrared divergence by using the factorization method.

The paper is organized as followings. In Sec. II, we calculate the decay constants of the B and B_s mesons. The branching ratios of leptonic decays of B meson are also calculated and compared with experimental data. In Sec. III, the matrix element between B meson and vacuum state, which defines the distribution amplitudes (DAs), is studied. The analytical form of the matrix element and DAs are obtained and figures are shown as illustrations. We finally obtain a compact expression for the matrix element. Section IV is devoted to the study of the pure leptonic decay of the B-mesons up to one-loop level in QCD and Sec. V is for the conclusion and discussion.

II. DECAY CONSTANTS OF B AND B_s MESONS

Recently, the spectra of heavy-light quark-antiquark system have been studied in the relativistic potential model

*sunhk@mail.nankai.edu.cn
†yangmz@nankai.edu.cn

in our previous works [20–22], where hyperfine interactions are included [21,22]. The whole spectra of B and D system are in well agreement with experimental measurements. Hence in this work, we extend our previous works [21,22] by studying the decay properties of B meson with the wave functions obtained in the relativistic potential model. We study the decay constants of B and B_s mesons at first, and then give a compact form of distribution amplitudes of B-meson, which shall be useful for studying B decays.

The decay constant of a pseudoscalar meson is defined by the matrix element of the axial current between the meson and the vacuum state

$$\langle 0|\bar{q}\gamma^{\mu}\gamma^{5}Q|P\rangle = if_{P}P^{\mu} \tag{1}$$

where the axial current is composed of a light antiquark field $\bar{q}$ and a heavy quark field Q.

The pseudoscalar meson as a bound state of a quark and antiquark system can be described by [19,20],

$$\begin{aligned}|P(\vec{P})\rangle = &\frac{1}{\sqrt{N_L}}\frac{1}{\sqrt{3}}\sum_{i}\int \mathrm{d}^3k_q\mathrm{d}^3k_Q\delta^{(3)}(\vec{P}-\vec{k}_q-\vec{k}_Q)\Psi_0(\vec{k}_q)\\ &\times\frac{1}{\sqrt{2}}[c^{i\dagger}(\vec{k}_Q,\uparrow)b^{i\dagger}(\vec{k}_q,\downarrow)\\ &-c^{i\dagger}(\vec{k}_Q,\downarrow)b^{i\dagger}(\vec{k}_q,\uparrow)]|0\rangle\end{aligned} \tag{2}$$

where N_L is the normalization factor, and the normalization conditions will be shown explicitly below. i stands for the QCD color index and $\frac{1}{\sqrt{3}}$ is the corresponding normalization factor. The factor $\frac{1}{\sqrt{2}}$ is the normalization factor for the quark spin states which are indexed by up or down arrows. Inside the square parenthesis, $b^{i\dagger}$ and $c^{i\dagger}$ are the creation operators of the light antiquark $\bar{q}$ and the heavy quark Q, respectively.

The function $\Psi_0(\vec{k}_q)$ is the normalized wave function of the pseudoscalar meson at ground state in the momentum space, which describes the wave function of the quark and antiquark constituents in a meson. It is noted here that these quark constituents are the effective quarks carrying a gluon cloud and therefore the quarks have constituent masses [54].

The wave function can be obtained by solving the Schrödinger type wave equation with relativistic dynamics

$$(H_0 + H')\Psi(\vec{r}) = E\Psi(\vec{r}), \tag{3}$$

where $H_0 + H'$ is the effective Hamiltonian (its explicit expression can be found in Ref. [22]) and E is the energy of the meson. The first term H_0 contains the kinetic part and the effective potential which is taken as a combination of a Coulomb term and a linear confining term inspired by QCD [34,55,56].

The second term H' is the spin-dependent part of the Hamiltonian including contributions of one-gluon-exchange diagram in the nonrelativistic approximation [34,57] and new terms which account for contributions of nonperturbative dynamics in the bound state system and relativistic corrections for the light quark in the heavy meson [21,22].

The normalization conditions for wave function are

$$\int \mathrm{d}^3k|\Psi_0(\vec{k})|^2 = 1, \tag{4a}$$

$$\{c(\vec{k},s), c^{\dagger}(\vec{k}',s')\} = \delta_{ss'}\delta^{(3)}(\vec{k}-\vec{k}'), \tag{4b}$$

$$\langle P(\vec{P})|P(\vec{P}')\rangle = (2\pi)^3 2E\delta^{(3)}(\vec{P}-\vec{P}'). \tag{4c}$$

Note that we omit the color index of the operator c and use s, s' to denote the spin states. Substituting Eq. (2) into Eq. (4c) and using Eq. (4a) and Eq. (4b), we can obtain the normalization factor

$$N_L = \frac{1}{(2\pi)^3 2E}. \tag{5}$$

The wave function has been solved numerically in our previous work [22]. For B meson, the wave function can be expressed by

$$\Psi_0(\vec{k}) = \frac{\varphi_0(|\vec{k}|)}{|\vec{k}|}Y_{00}(\theta,\phi) \tag{6}$$

where $\varphi_0(|\vec{k}|)$ is the reduced wave function. The numerical result of $\varphi_0(|\vec{k}|)$ can be shown in Fig. 1.

Since it is convenient to have an analytical form of the wave function $\Psi_0(\vec{k})$ for the numerical calculation, we fit the wave function obtained in our previous work [22] with an exponential function and finally obtain the fitted form for the $B_{(s)}$ meson wave function with combined theoretical uncertainties as

$$\Psi_0(\vec{k}) = a_1 e^{a_2|\vec{k}|^2 + a_3|\vec{k}| + a_4}, \tag{7}$$

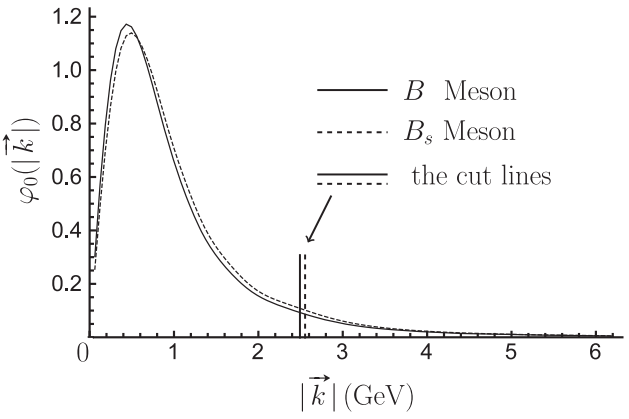

FIG. 1. Reduced wave functions for B-meson.

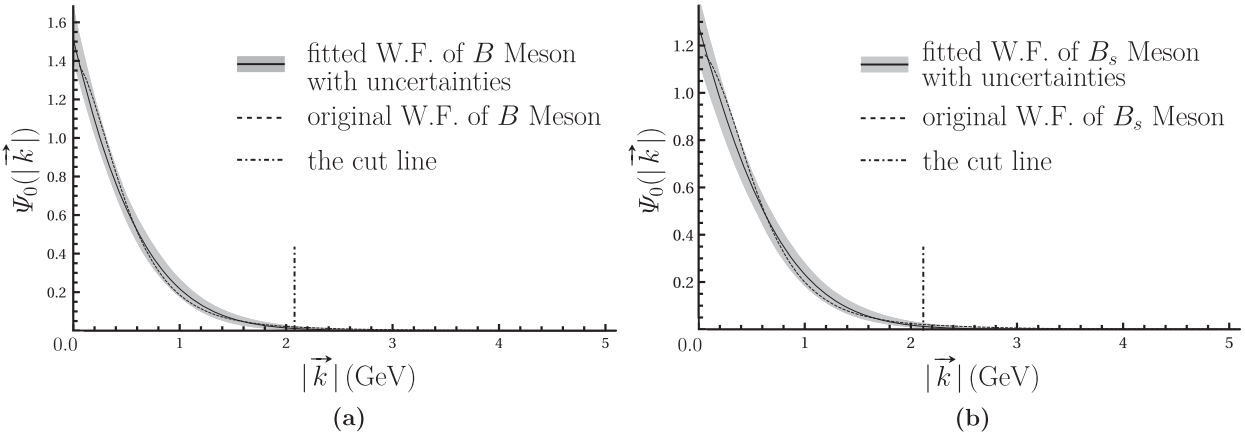

FIG. 2. The wave functions (W.F.) of B-meson.

where the parameters including uncertainties for B meson are

$$a_1 = 4.55^{+0.40}_{-0.30}\ \mathrm{GeV}^{-3/2}, \quad a_2 = -0.39^{+0.15}_{-0.20}\ \mathrm{GeV}^{-2};$$
$$a_3 = -1.55 \pm 0.20\ \mathrm{GeV}^{-1}, \quad a_4 = -1.10^{+0.10}_{-0.05}, \tag{8}$$

and for B_s meson:

$$a_1 = 1.60^{+0.15}_{-0.18}\ \mathrm{GeV}^{-3/2}, \quad a_2 = -0.43^{+0.15}_{-0.10}\ \mathrm{GeV}^{-2};$$
$$a_3 = -1.28^{+0.18}_{-0.20}\ \mathrm{GeV}^{-1}, \quad a_4 = -0.22^{+0.06}_{-0.08}. \tag{9}$$

The uncertainties for the parameters ensure that the deviation of the wave function from its central value is approximately about 8%. The illustrations for the fit of the wave functions are shown in Fig. 2, where the grey bands denote the relevant uncertainties for the wave functions of B and B_s mesons.

In the calculation of the decay constants, four-momentum conservation should hold

$$k_q + k_Q = P, \tag{10}$$

where $k_{q,Q}$ and P are the momenta of the quark constituents and the meson, respectively.

With the restriction above, we consider the Altarelli-Cabibbo-Corbo-Maiani-Martinelli (ACCMM) scenario [58,59], where the light quark is kept on-shell, while the heavy quark off-shell,

$$E_q + E_Q = m_P, \tag{11a}$$

$$E_q^2 = m_q^2 + |\vec{k}|^2, \tag{11b}$$

$$m_Q^2(\vec{k}) = E_Q^2 - |\vec{k}|^2. \tag{11c}$$

Equation (11a) is the energy conservation in the meson rest frame. We assume that the running mass of the heavy quark must be positive $m_Q(\vec{k}) \geq 0$. Thus the actual range of the momentum $|\vec{k}|$ is restricted under a particular value, which is shown as the cut lines in Figs. 1 and 2.

Substituting Eq. (2) into Eq. (1) in the rest frame and contracting the quark (antiquark) creation operators with the annihilation operators in the quark field of the axial current $\bar{q}\gamma^\mu\gamma^5 Q$, we obtain

$$f_P = \sqrt{\frac{3}{(2\pi)^3 m_P}} \int \mathrm{d}^3k \Psi_0(\vec{k}) \frac{(E_q + m_q)(E_Q + m_Q) - |\vec{k}|^2}{\sqrt{E_q E_Q (E_q + m_q)(E_Q + m_Q)}}, \tag{12}$$

where the integral over the variable $\vec{k}$ should be limited in the finite range according to Eqs. (11a)–(11c).

The parameters used in this work are [22]

$$m_s = 0.32\ \mathrm{GeV}, \quad m_u = m_d = 0.06\ \mathrm{GeV},$$
$$m_b = 4.99\ \mathrm{GeV}, \tag{13}$$

and the mesons' masses are taken from PDG [46]

$$m_B = 5.28\ \mathrm{GeV} \quad m_{B_s} = 5.37\ \mathrm{GeV}. \tag{14}$$

The errors are estimated by varying the parameters in the allowed ranges. The total errors are around 7% for the decay constants of B and B_s mesons. We also calculate the ratio of the decay constants of B and B_s mesons f_{B_s}/f_B. The final results obtained are

$$f_B = 219 \pm 15\ \mathrm{MeV}, \quad f_{B_s} = 266 \pm 19\ \mathrm{MeV},$$
$$f_{B_s}/f_B = 1.21 \pm 0.09. \tag{15}$$

During past decades, many theoretical methods or models have been developed for the calculation of the B-meson decay constants. In this paper, we list some of the results for

TABLE I. Theoretical results of the decay constants of B-mesons.

Reference	Method	f_B (MeV)	f_{B_s} (Mev)	f_{B_s}/f_B
this work	RPM[a]	219 ± 15	266 ± 19	1.21 ± 0.09
Colangelo 91 [35]	RPM	230 ± 35	245 ± 37	1.07 ± 0.17
Cvetič 04 [31]	QM BS[c]	196 ± 29	216 ± 32	1.10 ± 0.18
Badalian 07 [32]	FCM[f]	182 ± 8	216 ± 8	1.19 ± 0.03
Hwang 09 [60]	LFQM[e]	204 ± 31	270.0 ± 42.8	1.32 ± 0.08
HPQCD 11 [41]	LQCD $(2+1)$[d]	–	$225 \pm 3 \pm 3$	–
FNAL/MILC 11 [42]	LQCD $(2+1)$	$196.9 \pm 5.5 \pm 7.0$	$242.0 \pm 5.1 \pm 8.0$	$1.229 \pm 0.013 \pm 0.023$
HPQCD 12 [44]	LQCD $(2+1)$	$191 \pm 1 \pm 8$	$228 \pm 3 \pm 10$	$1.188 \pm 0.012 \pm 0.013$
Narison 12 [27]	QCD SR[b]	206 ± 7	234 ± 5	1.14 ± 0.03
Gelhausen 13 [28]	QCD SR	207^{+17}_{-9}	242^{+17}_{-12}	$1.17^{+0.03}_{-0.04}$
HPQCD 13 [45]	LQCD $(2+1+1)$	184 ± 4	224 ± 5	1.217 ± 0.008
ETM 13 [61]	LQCD $(2+1+1)$	196 ± 9	235 ± 9	1.201 ± 25
Aoki 14 [62]	LQCD $(2+1)$	$218.8 \pm 6.4 \pm 30.8$	$263.5 \pm 4.8 \pm 36.7$	$1.193 \pm 0.020 \pm 0.044$
RBC/UKQCD 14 [63]	LQCD $(2+1)$	$195.6 \pm 6.4 \pm 13.3$	$235.4 \pm 5.2 \pm 11.1$	$1.223 \pm 0.014 \pm 0.070$
Wang 15 [64]	QCD SR	194 ± 15	231 ± 16	1.19 ± 0.10

[a]Relativistic potential model.
[b]QCD sum rules.
[c]Quark model based on Bethe-Salpeter equation.
[d]lattice-QCD with dynamical quark flavors N_f in the parentheses.
[e]Light-front quark model.
[f]Field correlator method.

comparison in Table I, where one can see that our results are consistent with most of the theoretical predictions.

The branching ratio of the leptonic decay of B meson can be calculated by the following formula

$$\mathcal{B}(B^{\pm} \to l^{\pm}\nu) = \frac{G_F^2 m_l^2 m_B}{8\pi}\left(1-\frac{m_l^2}{m_B^2}\right)^2 f_B^2 |V_{ub}|^2 \tau_B, \quad (16)$$

where G_F is the Fermi constant, V_{ub} the Cabibbo-Kobayashi-Maskawa (CKM) matrix element, m_B and m_l the masses of $B^{\pm}$ meson and lepton, respectively, and τ_B is the life time of $B^{\pm}$ meson.

In this work, we obtain

$$\mathcal{B}(B^+ \to e^+\nu_e) = (1.17 \pm 0.18) \times 10^{-11}, \quad (17a)$$

$$\mathcal{B}(B^+ \to \mu^+\nu_\mu) = (5.01 \pm 0.78) \times 10^{-7}, \quad (17b)$$

$$\mathcal{B}(B^+ \to \tau^+\nu_\tau) = (1.41 \pm 0.22) \times 10^{-4}, \quad (17c)$$

where the errors mainly come from the uncertainties of the decay constants f_B and the CKM matrix element $|V_{ub}|$ [46]

$$|V_{ub}| = (4.09 \pm 0.39) \times 10^{-3}. \quad (18)$$

TABLE II. Experimental results for $\mathcal{B}(B^+ \to \tau^+\nu_\tau)$.

Experiment	Tag	$\mathcal{B}$ (units of 10^{-4})
Belle [47]	Hadronic	$0.72^{+0.27}_{-0.25} \pm 0.11$
Belle [48]	Semileptonic	$1.25 \pm 0.28 \pm 0.27$
BABAR [49]	Hadronic	$1.83^{+0.53}_{-0.49} \pm 0.24$
BABAR [50]	Semileptonic	$1.7 \pm 0.8 \pm 0.2$

The branching ratio of $B \to \tau^+\nu_\tau$ channel has been measured by Belle and *BABAR* collaborations [47–50]. The results are shown in Table II.

Taking the large uncertainties of the experimental data into consideration, our predicted branching ratio of the decay channel $B^+ \to \tau^+\nu_\tau$ [Eq. (17c)] is consistent with the experimental results.

As an upgrade of the Belle/KEKB experiment, the Belle II/SuperKEKB will start taking data from 2018. With a designed luminosity 8×10^{35} cm^{-2} s^{-1}, which is about 40 times larger than its predecessor, data sample corresponding to 50 ab^{-1} will be accumulated within five years of operation [53]. It is expected to reduce both the statistical and systematic errors of the $B^+ \to \tau^+\nu_\tau$ decay mode by a factor about 7 [65].

III. B-MESONS DISTRIBUTION AMPLITUDES

Based on the success of our predictions on the mass spectra [20–22] and the decay constants of B-mesons, we continue to study of the matrix element of B meson which defines the DAs. The matrix element and DAs are generally used in studying hadronic decays of B meson.

Generalizing the current in the definition of the decay constant in Eq. (1) from local to nonlocal operators and making use of Fierz identity, we obtain the matrix element between the B meson and the vacuum state in coordinate space

$$\tilde{\Phi}_{\alpha\beta}(z) \equiv \langle 0|\bar{q}_\beta(z)[z,0]Q_\alpha(0)|\bar{B}(P)\rangle \tag{19a}$$

$$\begin{aligned}&= \frac{1}{4}\langle 0|\bar{q}(z)Q(0)|\bar{B}\rangle I_{\alpha\beta} + \frac{1}{4}\langle 0|\bar{q}(z)\gamma^5 Q(0)|\bar{B}\rangle(\gamma^5)_{\alpha\beta} \\ &+ \frac{1}{8}\langle 0|\bar{q}(z)\sigma^{\mu\nu}\gamma^5 Q(0)|\bar{B}\rangle(\sigma_{\mu\nu}\gamma^5)_{\alpha\beta} \\ &+ \frac{1}{4}\langle 0|\bar{q}(z)\gamma^\mu Q(0)|\bar{B}\rangle(\gamma_\mu)_{\alpha\beta} \\ &- \frac{1}{4}\langle 0|\bar{q}(z)\gamma^\mu\gamma^5 Q(0)|\bar{B}\rangle(\gamma_\mu\gamma^5)_{\alpha\beta},\end{aligned} \tag{19b}$$

where $\sigma^{\mu\nu} = \frac{i}{2}[\gamma^\mu, \gamma^\nu]$, and $[z,0]$ stands for the path-ordered exponential, which is called Wilson line that connects the point 0 and z. The definition of Wilson line is

$$[z,0] \equiv \mathrm{P}\exp\left(i\int_0^z \mathrm{d}x^\mu A_\mu(x)\right). \tag{20}$$

According to discrete symmetries of C, P and T, the matrix elements in the right-hand side of Eq. (19b) are related to four DAs $\tilde{\phi}_i$ $(i = P, T, A1, A2)$ as defined in Ref. [10]

$$\langle 0|\bar{q}(z)Q(0)|\bar{B}\rangle = 0, \tag{21a}$$

$$\langle 0|\bar{q}(z)\gamma^5 Q(0)|\bar{B}\rangle = -if_B m_B\tilde{\phi}_P, \tag{21b}$$

$$\langle 0|\bar{q}(z)\sigma^{\mu\nu}\gamma^5 Q(0)|\bar{B}\rangle = -if_B\tilde{\phi}_T(P^\mu z^\nu - P^\nu z^\mu), \tag{21c}$$

$$\langle 0|\bar{q}(z)\gamma^\mu Q(0)|\bar{B}\rangle = 0, \tag{21d}$$

$$\langle 0|\bar{q}(z)\gamma^\mu\gamma^5 Q(0)|\bar{B}\rangle = f_B(i\tilde{\phi}_{A1}P^\mu - m_B\tilde{\phi}_{A2}z^\mu), \tag{21e}$$

where the DAs $\tilde{\phi}_i$ are functions of the coordinate z. In our scenario, we calculate these five matrix elements in the B-meson rest frame by using the B meson state defined in Eq. (2). We confirmed that the matrix elements in Eq. (21a) and Eq. (21c) are indeed zero

$$\langle 0|\bar{q}(z)Q(0)|\bar{B}\rangle = \langle 0|\bar{q}(z)\gamma^\mu Q(0)|\bar{B}\rangle = 0. \tag{22}$$

For the pseudoscalar DA in Eq. (21b), we obtain

$$\begin{aligned}\tilde{\phi}_P(z) = N_B\int \mathrm{d}^3k\Psi_0(\vec{k}) \\ \times\frac{-[(E_q+m_q)(E_Q+m_Q)+|\vec{k}|^2]}{\sqrt{E_qE_Q(E_q+m_q)(E_Q+m_Q)}}e^{-ik_q\cdot z},\end{aligned} \tag{23}$$

where $k_q^\mu = (E_q, \vec{k})$ is the four-momentum of the light quark in the meson rest frame, and

$$N_B \equiv \frac{i}{f_B}\sqrt{\frac{3}{(2\pi)^3 m_B}}. \tag{24}$$

It should be understood that the wave function $\Psi_0(\vec{k})$ may have an arbitrary phase which can be adjusted to obtain a positive real decay constant according to the definition in Eq. (1).

For the other DAs in Eqs. (21c) and (21e) (the detailed derivation can be found in Appendix A), we introduce two functions A_T and A at first,

$$A_T(k^1,k^2,k^3) \equiv \Psi_0(\vec{k})\frac{E_Q+m_Q+E_q+m_q}{\sqrt{E_qE_Q(E_q+m_q)(E_Q+m_Q)}}, \tag{25a}$$

$$A(k^1,k^2,k^3) \equiv \Psi_0(\vec{k})\frac{E_Q+m_Q-E_q-m_q}{\sqrt{E_qE_Q(E_q+m_q)(E_Q+m_Q)}}, \tag{25b}$$

where k^1, k^2, k^3 are the components of the light quark momentum $\vec{k}$, i.e., $\vec{k} = (k^1,k^2,k^3)$. Then we obtain the DAs as

$$\tilde{\phi}_T(z) = N_B\int \mathrm{d}^3k\left[\frac{1}{3}\sum_i\int_0^{k^i} A_T(\eta,\ldots)\eta\mathrm{d}\eta\right]e^{-ik_q\cdot z}, \tag{26a}$$

$$\tilde{\phi}_{A2}(z) = N_B\int \mathrm{d}^3k\left[\frac{1}{3}\sum_i\int_0^{k^i} A(\eta,\ldots)\eta\mathrm{d}\eta\right]e^{-ik_q\cdot z}, \tag{26b}$$

$$\begin{aligned}\tilde{\phi}_{A1}(z) = -N_B\int \mathrm{d}^3k e^{-ik_q\cdot z} \\ \cdot\left[\Psi_0(\vec{k})\frac{(E_q+m_q)(E_Q+m_Q)-|\vec{k}|^2}{\sqrt{E_qE_Q(E_q+m_q)(E_Q+m_Q)}}\right. \\ \left. + E_qA(k^1,k^2,k^3)\right].\end{aligned} \tag{26c}$$

For the details of the summation in the square parentheses containing the ellipsis, see Eq. (A3).

Now, with Eqs. (21a)–(21e), the matrix element for B-meson in Eq. (19a) can be rewritten as

$$\begin{aligned}\tilde{\Phi}_{\alpha\beta}(z) = \frac{-if_B}{4}\left\{\left[m_B\tilde{\phi}_P + \frac{1}{2}\tilde{\phi}_T(P^\mu z^\nu - P^\nu z^\mu)\sigma_{\mu\nu}\right.\right. \\ \left.\left. + (\tilde{\phi}_{A1}P^\mu + im_B\tilde{\phi}_{A2}z^\mu)\gamma_\mu\right]\gamma^5\right\}_{\alpha\beta},\end{aligned} \tag{27}$$

where the DAs are given in Eqs. (23) and (26a)–(26c).

In order to obtain the expressions of the DAs in momentum space, we make use of the amplitude of a decay process which can be expressed as a convolution [11]

$$F = \int \mathrm{d}^4 z \tilde{\Phi}_{\alpha\beta}(z) \tilde{T}_{\beta\alpha}(z). \tag{28}$$

Substituting Eq. (27) into Eq. (28) and with a few steps of calculation (see Appendix B for details), we obtain

$$\Phi_{\alpha\beta}(l) = \left\{ \frac{-if_B m_B}{4} \left[\phi_P(l) + \frac{i}{2} \phi_T(l) \sigma_{\mu\nu} \left(v^\mu \frac{\partial}{\partial l_\nu} - v^\nu \frac{\partial}{\partial l_\mu} \right) + \left(\phi_{A1}(l) \not{v} - \phi_{A2}(l) \gamma_\mu \frac{\partial}{\partial l_\mu} \right) \right] \gamma^5 \right\}_{\alpha\beta} \tag{29}$$

and

$$F = \int \mathrm{d}^3 l \Phi_{\alpha\beta}(l) T_{\beta\alpha}(l)|_{l^2 = m_q^2}. \tag{30}$$

It is understood that the derivative $\frac{\partial}{\partial l_{\mu,\nu}}$ in Eq. (29) (which is called the momentum space projector [11,66]) acts on the hard-scattering kernel $T_{\beta\alpha}(l)$ before $l = k_q$ is taken. For the DAs in the momentum space, we obtain

$$\phi_P(k_q^\mu) = -N_B \frac{(E_q + m_q)(E_Q + m_Q) + |\vec{k}|^2}{\sqrt{E_q E_Q (E_q + m_q)(E_Q + m_Q)}} \Psi_0(\vec{k}), \tag{31a}$$

$$\phi_T(k_q^\mu) = \frac{N_B}{3} \sum_i \int_0^{k^i} A_T(\eta, \ldots) \eta \mathrm{d}\eta, \tag{31b}$$

$$\phi_{A2}(k_q^\mu) = \frac{N_B}{3} \sum_i \int_0^{k^i} A(\eta, \ldots) \eta \mathrm{d}\eta, \tag{31c}$$

$$\phi_{A1}(k_q^\mu) = -N_B \left[\Psi_0(\vec{k}) \frac{(E_q + m_q)(E_Q + m_Q) - |\vec{k}|^2}{\sqrt{E_q E_Q (E_q + m_q)(E_Q + m_Q)}} + E_q A(k^1, k^2, k^3) \right], \tag{31d}$$

In general, these DAs play an important role in the study of the B-meson decays [13]. Thus it is necessary and useful to give an numerical illustration of them.

For simplicity, we take $\vec{k} = (0, 0, k^3)$ and the DAs as functions of $|k^3|$ are shown in Fig. 3. The grey bands are the possible uncertainties caused by the uncertainty of the wave function. In the heavy-quark limit, one can obtain that one of the axial-vector DA ϕ_{A2} is equal to the axial-tensor DA ϕ_T [10]. For our results, as shown in Figs. 3(c) and (e), (3d) and (3f), these two DAs are indeed very close, which indicate that our scenario is reasonable and their difference reflects the influence of the finite heavy-quark mass.

One can also see that the figures for B and B_s mesons are very similar, but in detail, for the same values of $|k^3|$, the absolute values of the DAs of B meson are always a bit larger than that of B_s meson. This is consistent with the fact that the DAs are inversely proportional to the square root of the decay constants and masses.

In addition, the light-cone coordinate is widely used in the study of the DAs, for example, the works in Refs. [11,13,18,66–69] and references therein, where the DAs depend on a single variable k_+ or k_-, which are the light-cone projections of the momentum of the light antiquark in the rest frame of the meson. The definitions of the light-cone projections of the momentum of the light antiquark are

$$k_\pm = \frac{E_q \pm k^3}{\sqrt{2}}, \qquad k_\perp^\mu = (0, k^1, k^2, 0) \tag{32}$$

Performing the integration over the transverse momentum $k_\perp$, we can obtain the light-cone distribution amplitudes (LCDAs) in our scenario. Usually, the $k_\perp$-integral is restricted by a scale μ, i.e., $|k_\perp| < \mu$ [2,70]. In our model, the wave function is spherically symmetric with respect to k^1, k^2, and k^3. The integral region of the $k_\perp$ has an upper limit, which is determined by Eqs. (11a)–(11c). The upper limits are shown clearly by the cut lines in Fig. 1.

The distribution amplitude ϕ_{A1} as a function of k_+ is shown in Fig. 4. ϕ_{A1} is relevant to the LCDA ϕ_B^+ in the heavy quark limit, which is generally used in the study of B decays. Our results are consistent with the general analysis given in Ref. [13].

Next we try to give a compact form of the matrix element $\tilde{\Phi}_{\alpha\beta}(z) = \langle 0|\bar{q}_\beta(z)[z,0]Q_\alpha(0)|\bar{B}(P)\rangle$. Substituting Eq. (23) and Eqs. (26a)–(26c) into Eq. (19b) and after a few steps of simplification, we obtain

$$\tilde{\Phi}_{\alpha\beta}(z) = \frac{-1}{4} \sqrt{\frac{3m_B}{(2\pi)^3}} \int \mathrm{d}^3 k \frac{\Psi_0(\vec{k}) e^{-ik_q \cdot z}}{\sqrt{E_q E_Q (E_q + m_q)(E_Q + m_Q)}} \times \left\{ \begin{pmatrix} b \\ c \end{pmatrix} \begin{pmatrix} c & a \end{pmatrix} \right\}_{\alpha\beta} \quad \text{(D.R.)}$$

$$= \frac{-1}{4} \sqrt{\frac{3m_B}{(2\pi)^3}} \int \mathrm{d}^3 k \cdot \tag{33a}$$

$$\frac{\Psi_0(\vec{k}) e^{-ik_q \cdot z}}{\sqrt{E_q E_Q (E_q + m_q)(E_Q + m_Q)}} \times \left\{ \begin{pmatrix} b - c \\ b + c \end{pmatrix} \begin{pmatrix} c - a & c + a \end{pmatrix} \right\}_{\alpha\beta} \quad \text{(W.R.)}. \tag{33b}$$

where a, b, and c are three 2×2 matrices, which are defined as

$$a = (E_q + m_q) I_{2\times 2}, \quad b = (E_Q + m_Q) I_{2\times 2}, \quad c = \vec{k} \cdot \vec{\sigma}$$

and $\vec{\sigma}$ is the Pauli matrix. These two expressions in Eqs. (33a) and (33b) are derived with different representations of the gamma matrix γ^μ. The label D. R. denotes Dirac representation, and W. R. Weyl representation.

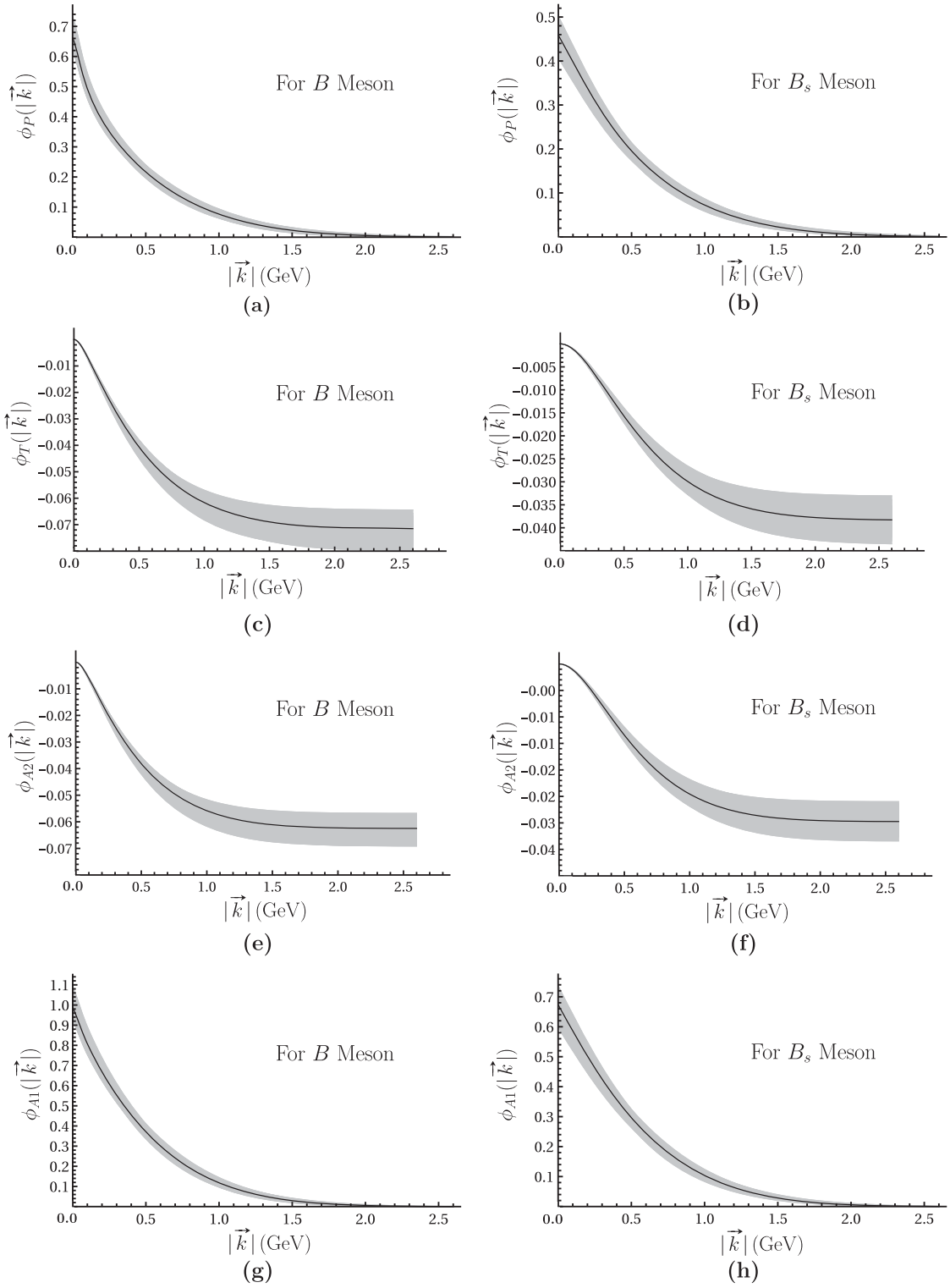

FIG. 3. Distribution amplitudes as functions of $|k^3|$, where the grey bands are uncertainties caused by the wave function.

For simplicity, we define

$$K(\vec{k}) \equiv \frac{-N_B \Psi_0(\vec{k})}{\sqrt{E_q E_Q (E_q + m_q)(E_Q + m_Q)}}. \tag{34}$$

Then the convolution formula of Eq. (30) can be rewritten as

$$F = \int \mathrm{d}^3 k \frac{-i f_B m_B}{4} K(\vec{k}) \left\{ \begin{pmatrix} b \\ c \end{pmatrix} \begin{pmatrix} c & a \end{pmatrix} \right\}_{\alpha\beta} T_{\beta\alpha}(k_q)|_{k_q^2 = m_q^2} \tag{35}$$

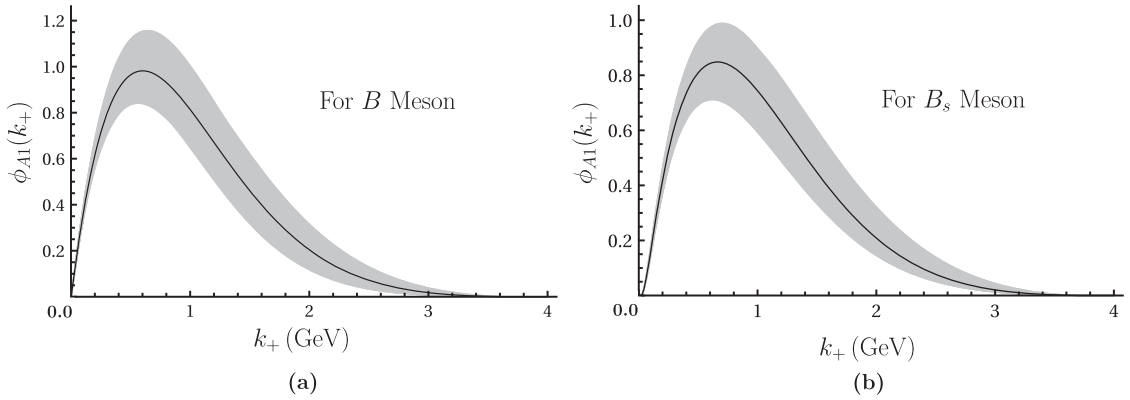

FIG. 4. Distribution amplitudes as functions of k_+, where the grey bands are uncertainties caused by the wave function.

where the spinor matrices are given in Dirac representation (D. R.).

Next we introduce two light-like vectors $n_\pm^\mu=(1,0,0,\mp1)$ and define $\not{n}_+ \equiv n_+^\mu\gamma_\mu = \left(\begin{smallmatrix}1 & \sigma^3\\ -\sigma^3 & -1\end{smallmatrix}\right)$, $\not{n}_- \equiv n_-^\mu\gamma_\mu = \left(\begin{smallmatrix}1 & -\sigma^3\\ \sigma^3 & -1\end{smallmatrix}\right)$. With these two vectors $n_\pm^\mu$, the matrix element $\Phi_{\alpha\beta}(k_q^\mu)$ can be expressed in another form

$$\begin{aligned}\Phi_{\alpha\beta}(k_q^\mu)=&\frac{-if_Bm_B}{4}K(\vec{k})\left\{\begin{pmatrix}b\\c\end{pmatrix}(c\ \ a)\right\}_{\alpha\beta}\\ =&\frac{-if_Bm_B}{4}K(\vec{k})\cdot\left\{(E_Q+m_Q)\frac{1+\not{v}}{2}\left[\left(\frac{k_+}{\sqrt{2}}+\frac{m_q}{2}\right)\not{n}_+\right.\right.\\ &\left.+\left(\frac{k_-}{\sqrt{2}}+\frac{m_q}{2}\right)\not{n}_- -k_\perp^\mu\gamma_\mu\right]\gamma^5\\ &-(E_q+m_q)\frac{1-\not{v}}{2}\left[\left(\frac{k_+}{\sqrt{2}}-\frac{m_q}{2}\right)\not{n}_+\right.\\ &\left.\left.+\left(\frac{k_-}{\sqrt{2}}-\frac{m_q}{2}\right)\not{n}_- -k_\perp^\mu\gamma_\mu\right]\gamma^5\right\}_{\alpha\beta}.\end{aligned}\tag{36}$$

Compared with the commonly used results (for instance, see Eq. (109) in Ref. [11] and Eq. (2.48) in Ref. [18]), this new form includes the whole spinor structure of the momentum projector. The part containing $\frac{1+\not{v}}{2}$ is proportional to the heavy quark's mass and is the only term in the heavy quark limit. Since when the heavy-quark mass m_Q goes infinity, the contribution of other part in Eq. (36) will be relatively very small and can be ignored. Therefore, as we take the finite heavy-quark mass, the part with (E_q+m_q) will give extra contribution and may be an important correction in the study of B-meson decays.

IV. QCD ONE-LOOP CORRECTIONS TO LEPTONIC DECAYS OF B-MESON

In Sec. II, we study the leptonic decays of B meson at tree level. In this section, we extend this study by including QCD one-loop corrections. When considering one-loop corrections in QCD, if one naively calculate the loop diagrams, one will encounter not only ultraviolet divergence, but also infrared divergence. Factorization method can be applied to obtain the infrared-safe amplitude at the quark level. To obtain the infrared-safe transition amplitude at quark level, let us consider the free quark state $|\bar{u}^r(k)b^s(p-k)\rangle$ as the initial state at first. Factorization means that the matrix element of a physics transition process F^μ can be expressed as the convolution of the wave function of the initial state and the hard transition amplitude T

$$F^\mu = \Phi\otimes T \tag{37}$$

where the circle-time $\otimes$ denotes the convolution in Eq. (28), and μ denotes the Lorentz index that may appear in the physical transition matrix element. All the infrared contributions are absorbed into the wave function Φ, while the hard amplitude T is infrared safe.

In perturbation theory, the matrix element F^μ, which relevant to the quark transition process, the wave function Φ and the hard-scattering kernel T can all be expanded by the power of α_s. Therefore the factorization formula takes the form [71]

$$\begin{aligned}F^\mu &= F^{(0)\mu}+F^{(1)\mu}+\cdots=\Phi\otimes T\\ &=[\Phi^{(0)}\otimes T^{(0)}]+[\Phi^{(0)}\otimes T^{(1)}+\Phi^{(1)}\otimes T^{(0)}]+\cdots,\end{aligned}\tag{38}$$

where the superscripts (n)'s indicate the perturbation levels. After calculating both the matrix element $F^{(1)\mu}$ and the wave function $\Phi^{(1)}$ at one-loop order, one can extract the hard amplitude $T^{(1)}$ by using Eq. (38), that is

$$\Phi^{(0)}\otimes T^{(1)} = F^{(1)\mu}-\Phi^{(1)}\otimes T^{(0)}\tag{39}$$

At one-loop level, both the matrix element $F^{(1)\mu}$ and the wave function $\Phi^{(1)}$ are infrared divergent. Through the subtraction in the right-hand side of Eq. (39), the infrared divergence can be cancelled. Then the hard amplitude $T^{(1)}$ we get through Eq. (39) is infrared safe.

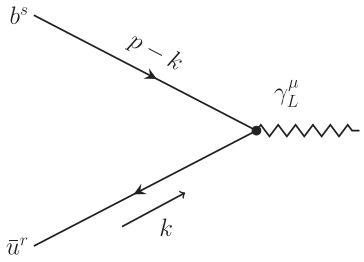

FIG. 5. Factorization at tree level.

At tree level, the factorization can be achieved straightforwardly and we show the results briefly at first. The matrix element F^μ at tree level, as shown in Fig. 5, can be obtained as

$$F_{b\bar{u}}^{(0)\mu} = \langle 0|\bar{u}\gamma_L^\mu b|\bar{u}^r(k)b^s(p-k)\rangle = \frac{1}{(2\pi)^3}\sqrt{\frac{m_u m_b}{k^0(p-k)^0}}\bar{v}^r(k)\gamma_L^\mu u^s(p-k) \quad (40)$$

where the coefficient $\frac{1}{(2\pi)^3}\sqrt{\frac{m_u m_b}{k^0(p-k)^0}}$ is from our convention, and $\bar{v}$ and u are the spinors of the quarks $\bar{u}$ and b, respectively. The superscripts r and s are the spin labels.

The wave function of the free quark state $|\bar{u}^r(k)b^s(p-k)\rangle$ at tree level is

$$\Phi_{\alpha\beta}^{(0)b\bar{u}}(\tilde{k}) = \int \mathrm{d}^4 z e^{i\tilde{k}\cdot z}\langle 0|\bar{u}_\beta(z)[z,0]b_\alpha(0)|\bar{u}^r(k)b^s(p-k)\rangle = \frac{1}{(2\pi)^3}\sqrt{\frac{m_u m_b}{k^0(p-k)^0}} \times (2\pi)^4\delta^{(4)}(\tilde{k}-k)\bar{v}_\beta^r(k)u_\alpha^s(p-k). \quad (41)$$

Matching the matrix element in Eq. (40) and the wave function in Eq. (41) into the factorization formula

$$F_{b\bar{u}}^{(0)\mu} = \int \frac{\mathrm{d}^4\tilde{k}}{(2\pi)^4}\Phi_{\alpha\beta}^{(0)b\bar{u}}(\tilde{k})T_{\beta\alpha}^{(0)}(\tilde{k}) = \frac{1}{(2\pi)^3}\sqrt{\frac{m_u m_b}{k^0(p-k)^0}}\bar{v}_\beta^r(k)T_{\beta\alpha}^{(0)}(k)u_\alpha^s(p-k), \quad (42)$$

we can obtain the hard-scattering kernel at tree level

$$T_{\beta\alpha}^{(0)}(k) = (\gamma_L^\mu)_{\beta\alpha}. \quad (43)$$

This tree-level result is independent of the quark momentum k. It plays an important role in the calculation of the hard amplitude at one-loop level.

Next we shall establish the factorization at one-loop level. The Feynman diagram for the matrix element $F^{(1)\mu}$ at one-loop level is shown as Fig. 6(a). The renormalization factor $\sqrt{Z_2^{\bar{u}}Z_2^b}$ must appear in the contribution of Fig. 6(a) due to the renormalization of the external quark fields, where $\sqrt{Z_2^{\bar{u}}}$ and $\sqrt{Z_2^b}$ are the renormalization constants of the external quark fields $\bar{u}$ and b, respectively. Since the factor $\sqrt{Z_2^b}$ and $\sqrt{Z_2^{\bar{u}}}$ correspond to the self-energy diagrams of the external quark b and $\bar{u}$, the factor $\sqrt{Z_2^{\bar{u}}Z_2^b}$ can be represented by the contributions of Fig. 6(b) and (c).

The contribution of Fig. 6(a) is

$$F_V^{(1)\mu} = \frac{1}{(2\pi)^3}\sqrt{\frac{m_u m_b}{k^0(p-k)^0}}(-ig_s^2)C_F\bar{v}^r(k) \cdot \int \frac{\mathrm{d}^4 l}{(2\pi)^4}\gamma^\rho \frac{1}{m_u-(\not{l}-\not{k})}\gamma_L^\mu \times \frac{1}{m_b-(\not{p}-\not{k}+\not{l})}\gamma_\rho\frac{1}{l^2}u^s(p-k), \quad (44)$$

where g_s is the strong coupling constant, and all the momenta of quarks and gluon are labelled in Fig. 6(a). The explicit result after the loop integration is given in Appendix C.

The contributions of Fig. 6(b) and (c) are

$$F_{bR}^{(1)\mu} = \frac{1}{2}(Z_2^b-1)F_{b\bar{u}}^{(0)\mu}, \quad F_{\bar{u}R}^{(1)\mu} = \frac{1}{2}(Z_2^{\bar{u}}-1)F_{b\bar{u}}^{(0)\mu}. \quad (45)$$

The renormalization constants (the explicit expressions are listed in Appendix C) are defined in terms of the one-particle irreducible (1PI) diagrams Σ by

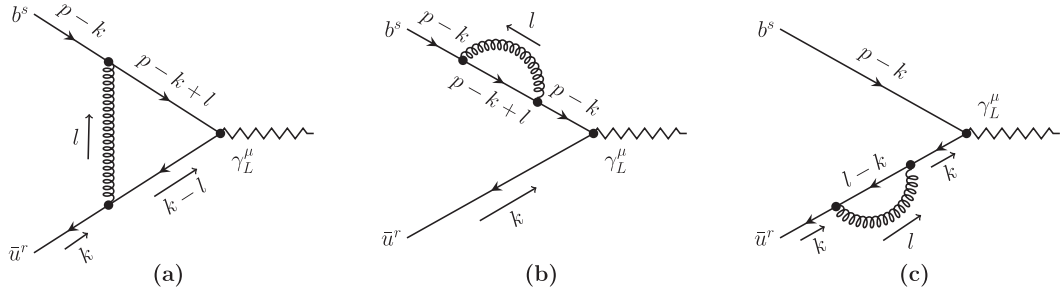

FIG. 6. Feynman diagrams at one-loop level for F.

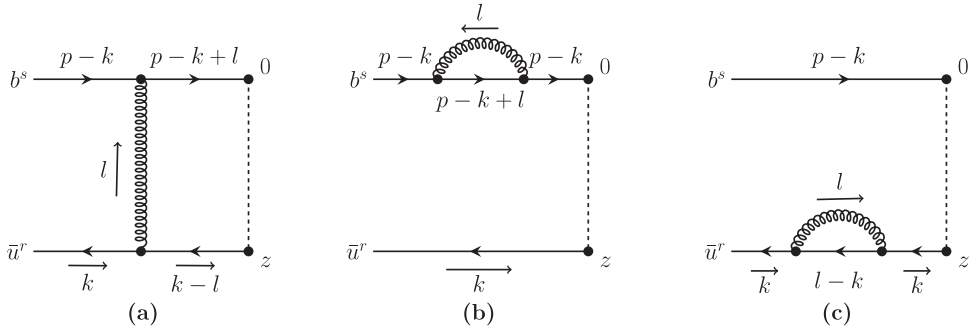

FIG. 7. Feynman diagrams at one-loop level for WF (1).

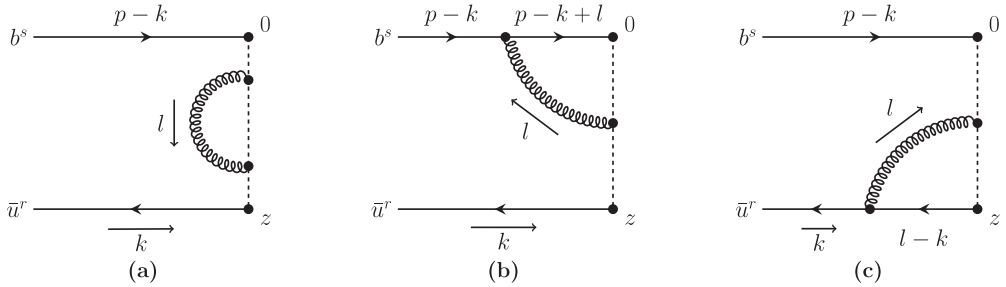

FIG. 8. Feynman diagrams at one-loop level for WF (2).

$$Z_2^{b,\bar{u}} = 1 + i\frac{\mathrm{d}\Sigma}{\mathrm{d}\not{p}}\bigg|_{\not{p}=m}. \tag{46}$$

The corrections for the wave functions at one-loop order contain 6 Feynman diagrams which have been divided into two groups. They are shown in Figs. 7 and 8. It will be shown later that, when the contribution of the diagrams in Fig. 8 is convoluted with the hard-transition kernel at tree level, the result will be zero.

The contribution of the diagram Fig. 7(a) to the wave function is

$$\Phi_{\alpha\beta}^{(1)V}(\tilde{k}) = (2\pi)^4\delta^{(4)}(l-k+\tilde{k})\frac{1}{(2\pi)^3}\sqrt{\frac{m_u m_b}{k^0(p-k)^0}}(-ig_s^2)C_F\int\frac{\mathrm{d}^4 l}{(2\pi)^4}\cdot\left[\bar{v}^r(k)\gamma^\rho\frac{1}{m_u-(\not{p}-\not{k})}\right]_\beta \times\left[\frac{1}{m_b-(\not{p}-\not{k}+\not{l})}\gamma_\rho\frac{1}{l^2}u^s(p-k)\right]_\alpha \tag{47}$$

and the contributions of the wave function renormalization of the heavy quark field [Fig. 7(b)] and the light quark field [Fig. 7(c)] are

$$\Phi_{\alpha\beta}^{(1)b} = \frac{1}{2}(Z_2^b-1)\Phi_{\alpha\beta}^{(0)b\bar{u}},\ \Phi_{\alpha\beta}^{(1)\bar{u}} = \frac{1}{2}(Z_2^{\bar{u}}-1)\Phi_{\alpha\beta}^{(0)b\bar{u}}. \tag{48}$$

Then it is straightforward to obtain the results after the convolution with the hard-scattering kernel at tree level $T_{\beta\alpha}^{(0)} = (\gamma_L^\mu)_{\beta\alpha}$ and we find that

$$F_V^{(1)\mu} = \Phi_{\alpha\beta}^{(1)V}\otimes T_{\beta\alpha}^{(0)}, \tag{49a}$$

$$F_{bR}^{(1)\mu} = \Phi_{\alpha\beta}^{(1)b}\otimes T_{\beta\alpha}^{(0)}, \tag{49b}$$

$$F_{\bar{u}R}^{(1)\mu} = \Phi_{\alpha\beta}^{(1)\bar{u}}\otimes T_{\beta\alpha}^{(0)}. \tag{49c}$$

It is noted that there are two scales in the above equations, i.e., the factorization scale μ_F in the wave functions $\Phi_{\alpha\beta}^{(1)b,\bar{u}}$ and the renormalization scale μ_R in the matrix element $F_{b,\bar{u}R}^{(1)\mu}$. Here we take $\mu_F = \mu_R$.

At last, we turn to the contributions of Feynman diagrams in Fig. 8. The contribution of Fig. 8(a) contains a gluon propagator both the starting and ending points being on the Wilson-line. In the light-cone approximation and working in the Feynman gauge, this propagator vanishes [71] since z is a null vector on the light-cone ($z^2 = 0$). As for our case, the result is still zero. First, we obtain

$$\Phi^{(1)0a}_{\alpha\beta}(\tilde{k}) = \frac{1}{(2\pi)^3}\sqrt{\frac{m_u m_b}{k^0(p-k)^0}}(ig_s^2)C_F\bar{v}^r(k)_\beta\int\frac{d^4l}{(2\pi)^4}\int d^4z e^{i\tilde{k}\cdot z}\cdot 2\int_0^1 dx z^\mu\int_0^x dy z^\nu e^{-ik\cdot z}e^{ixl\cdot z}e^{iy(-l)\cdot z}\frac{g_{\mu\nu}}{l^2}u^s(p-k)_\alpha \tag{50a}$$

$$= \frac{-i2g_s^2C_F}{(2\pi)^3}\sqrt{\frac{m_u m_b}{k^0(p-k)^0}}\bar{v}^r(k)_\beta\int\frac{d^4l}{(2\pi)^4}\int d^4z\int_0^1 dx\int_0^x dy\frac{e^{i(xl-k-yl)\cdot z}}{l^2}\left[\frac{\partial^2}{\partial\tilde{k}_\mu\partial\tilde{k}^\mu}e^{i\tilde{k}\cdot z}\right]u^s(p-k)_\alpha. \tag{50b}$$

In Eq. (50a) we make the substitution $x^\mu = xz^\mu$ and $y^\nu = yz^\nu$ in the Wilson-line.

Next, we can substitute Eq. (50b) into the convolution formula, and perform the partial integration. By noting that the hard-scattering kernel is a constant Dirac matrix, we can demonstrate

$$\Phi^{(1)0a}_{\alpha\beta}\otimes T^{(0)}_{\beta\alpha} = \int\frac{d^4\tilde{k}}{(2\pi)^4}\frac{i2g_s^2C_F}{(2\pi)^3}\sqrt{\frac{m_u m_b}{k^0(p-k)^0}}\bar{v}^r(k)_\beta\int\frac{d^4l}{(2\pi)^4}\int d^4z\int_0^1 dx\int_0^x dy\frac{e^{i(xl-k-yl)\cdot z}}{l^2}e^{i\tilde{k}\cdot z}\left[\frac{\partial^2}{\partial\tilde{k}_\mu\partial\tilde{k}^\mu}T^{(0)}_{\beta\alpha}\right]u^s(p-k)_\alpha$$
$$= 0. \tag{51}$$

For the other two diagrams in Fig. 8, the contribution of Fig. 8(b) is

$$\Phi^{(1)0b}_{\alpha\beta}(\tilde{k}) = \frac{i2g_s^2C_F}{(2\pi)^3}\sqrt{\frac{m_u m_b}{k^0(p-k)^0}}\int\frac{d^4l}{(2\pi)^4}\int d^4z\int_0^1 dx\frac{e^{i(xl-k)\cdot z}}{l^2}\bar{v}^r(k)_\beta\left[\frac{\partial}{\partial\tilde{k}_\rho}e^{i\tilde{k}\cdot z}\right]\left[\frac{1}{m_b-(\not{p}-\not{k}+\not{l})}\gamma_\rho u^s(p-k)\right]_\alpha \tag{52}$$

Then the convolution is

$$\Phi^{(1)0b}_{\alpha\beta}\otimes T^{(0)}_{\beta\alpha} = \int\frac{d^4\tilde{k}}{(2\pi)^4}\frac{-i2g_s^2C_F}{(2\pi)^3}\sqrt{\frac{m_u m_b}{k^0(p-k)^0}}\int\frac{d^4l}{(2\pi)^4}\int d^4z\int_0^1 dx\frac{e^{i(xl-k)\cdot z}}{l^2}$$
$$\times\bar{v}^r(k)_\beta e^{i\tilde{k}\cdot z}\left[\frac{\partial}{\partial\tilde{k}_\rho}T^{(0)}_{\beta\alpha}\right]\left[\frac{1}{m_b-(\not{p}-\not{k}+\not{l})}\gamma_\rho u^s(p-k)\right]_\alpha = 0. \tag{53}$$

Similarly, we can obtain that the contribution of Fig. 8(c) is also zero.

Finally, combining Eqs. (49a)–(49c), Eq. (51) and Eq. (53) together, we can demonstrate that $F^{(1)\mu}_{b\bar{u}} = \Phi^{(1)b\bar{u}}_{\alpha\beta}\otimes T^{(0)}_{\beta\alpha}$ and thus considering Eq. (39), the total contribution to the hard-scattering kernel at one-loop level $T^{(1)}_{\beta\alpha}$ is zero. Therefore the QCD one-loop corrections to the hard amplitude of the leptonic decay of B meson are zero in the factorization scheme.

A brief remark about this result should be given here. The vanishing of QCD one-loop correction to the hard decay amplitude of the pure leptonic decay of B meson does not mean that the naive calculation of the QCD one-loop correction diagrams in Fig. 6 will result in zero. The results in Eqs. (44), (45) and that given in Appendix C show that the contributions of these diagrams are not zero. They include both hard and infrared singularities. The infrared singularities come from the limit that the mass of the light quark approaches zero and/or the momentum of the gluon vanishes, i.e., $m_q \to 0$ and $l \to 0$. It has been known that a conserved current requires no renormalization because of gauge invariance [72]. Here the axial current $\bar{q}\gamma^\mu\gamma_5 b$ inducing the leptonic decay of B meson is partially conserved. Our calculation shows that the axial current as a composite operator still does not require renormalization. Only the external quark field renormalization is needed. Although the naive contributions of the diagrams in Fig. 6 are not zero, when QCD corrections to the wave function are also considered up to one-loop order, the infrared singularities and the hard contribution in the short-distance amplitude are simultaneously subtracted by that in the wave function by using Eq. (39). This implies that the infrared contribution in the short-distance amplitude can be absorbed into the wave function, and the hard terms are also absorbed and they will contribute to the evolution of the wave function.

The factorization and the result that the hard amplitude receives no QCD correction are proved up to one-loop order in this work. But we expect that this result may hold up to all orders in QCD, because the gluons are always restricted between the heavy quark and the light antiquark lines for both the cases of the QCD corrections to the wave function and that to the hard amplitude of the pure leptonic decay process. Therefore the subtraction may happen up to all orders in perturbative expansions. Then the formula that expresses the decay rate of the leptonic decay in Eq. (16) holds in all orders in perturbation theory. QCD corrections can only change the theoretical prediction to the decay constant.

V. DISCUSSION AND CONCLUSION

Using the wave function that is obtained in the relativistic potential model in our previous work [22], where the hyperfine interactions are included, the decay constants and pure leptonic decays of B meson are studied in this work. To keep the four-momentum conservation between the quark-antiquark pair and the meson, we use the ACCMM scenario [58,59] to treat the constituent quarks, where the heavy quark is taken to be off-shell, while the light antiquark is kept on shell. Compared with our earlier work [20], the difference is that the wave function used here is obtained by considering the hyperfine interactions in the wave equation, and the heavy quark is treated off-shell in the decay process. The off-shellness of the heavy quark can be explained as absorbing the effective effects of the gluon cloud around the heavy quark. With such a treatment, the branching ratios of leptonic decays of B meson obtained in this work are consistent with experimental data.

Based on the success of studying the leptonic decays of the B meson, we further obtain the distribution amplitudes for B meson both in coordinate and momentum space. The distribution amplitudes of B meson are widely used in the study of B-meson decays. In addition, we obtain another form of the nonlocal matrix element in Eq. (36). Considering the success of the ACCMM scenario in studying the leptonic decays, the heavy quark in the distribution amplitude needs to be treated to be off-shell to maintain the momentum and energy conservation. The new form of the nonlocal matrix element obtained in this work, Eqs. (33) or (33b) and Eq. (36) should be useful in the study of the semileptonic and nonleptonic B decays, where the longitudinal and transverse components are automatically included.

We finally study the QCD one-loop corrections within the frame work of the factorization approach. We find that, after subtracting the infrared divergence, the QCD one-loop corrections to the hard transition amplitude will be zero. This implies that the infrared contributions in the hard amplitude can be absorbed into the wave function and the hard terms originated from one-loop diagrams are also absorbed by the wave function and they will contribute to the evolution of the wave function. The formula expressing the leptonic decay rate of B meson in Eq. (16) is not affected by QCD corrections.

ACKNOWLEDGMENTS

This work is supported in part by the National Natural Science Foundation of China under Contract No. 11375088.

APPENDIX A: DERIVATION OF THE DISTRIBUTION AMPLITUDES $\tilde{\phi}_T(z)$, $\tilde{\phi}_{A1}(z)$, AND $\tilde{\phi}_{A2}(z)$

In this appendix, we give a brief derivation of the three distribution amplitudes presented in Eqs. (26a)–(26c). The direct result about $\tilde{\phi}_T(z)$ in Eq. (21c) is

$$\tilde{\phi}_T(z)z^i = iN_B\int \mathrm{d}^3k\Psi_0(\vec{k}) \times\frac{E_q+m_q+E_Q+m_Q}{\sqrt{E_qE_Q(E_q+m_q)(E_Q+m_Q)}}k^ie^{-ik_q\cdot z} \tag{A1}$$

where k^i stands for any components of momentum $\vec{k}$ and $N_B=\frac{i}{f_B}\sqrt{\frac{3}{(2\pi)^3m_B}}$. Note that $z_ie^{-ik_q\cdot z}=i\frac{\partial}{\partial k^i}e^{-ik_q\cdot z}$ and make use of $A_T(k^1,k^2,k^3)$ defined in Eq. (25),

$$A_T(k^1,k^2,k^3)k^1=\frac{\partial}{\partial k^1}\int_0^{k^1}A_T(\eta,k^2,k^3)\eta\mathrm{d}\eta \tag{A2a}$$

$$\Rightarrow\tilde{\phi}_T(z)z^1=N_B\int\mathrm{d}^3k \times\int_0^{k^1}A_T(\eta,k^2,k^3)\eta\mathrm{d}\eta(-z_1)e^{-ik_q\cdot z} \tag{A2b}$$

$$\Rightarrow\tilde{\phi}_T(z)=N_B \times\int\mathrm{d}^3k\left[\frac{1}{3}\sum_i\int_0^{k^i}A_T(\eta,\ldots)\eta\mathrm{d}\eta\right]e^{-ik_q\cdot z} \tag{A2c}$$

where Eq. (A2b) is derived from Eq. (A2a) by partial integration. The summation in the square parentheses is short for the following form

$$\begin{aligned}&\sum_i\int_0^{k^i}A_T(\eta,\ldots)\eta\mathrm{d}\eta\\&=\int_0^{k^1}A_T(\eta,k^2,k^3)\eta\mathrm{d}\eta+\int_0^{k^2}A_T(k^1,\eta,k^3)\eta\mathrm{d}\eta\\&\quad+\int_0^{k^3}A_T(k^1,k^2,\eta)\eta\mathrm{d}\eta.\end{aligned} \tag{A3}$$

The situation is similar for the derivation of $\tilde{\phi}_{A2}(z)$.

For the DA $\tilde{\phi}_{A1}(z)$, after substituting Eq. (26b) and Eq. (25b) into the equation Eq. (21e), we obtain

$$\tilde{\phi}_{A1}(z)=-N_B\int\mathrm{d}^3ke^{-ik_q\cdot z} \times\left[\Psi_0(\vec{k})\frac{(E_q+m_q)(E_Q+m_Q)-|\vec{k}|^2}{\sqrt{E_qE_Q(E_q+m_q)(E_Q+m_Q)}} +\frac{iz^0}{3}\sum_i\int_0^{k^i}A(\eta,\ldots)\eta\mathrm{d}\eta\right]. \tag{A4}$$

Using the same trick $iz^0e^{-ik_q\cdot z}=-\frac{\partial}{\partial E_q}e^{-ik_q\cdot z}$ and partial integration and noting that in our scenario $E_q^2-|\vec{k}|^2=m_q^2$, we get the final expression

$$\tilde{\phi}_{A1}(z) = -N_B \int \mathrm{d}^3k e^{-ik_q\cdot z} \times \left[\Psi_0(\vec{k})\frac{(E_q+m_q)(E_Q+m_Q)-|\vec{k}|^2}{\sqrt{E_qE_Q(E_q+m_q)(E_Q+m_Q)}} + E_qA(k^1,k^2,k^3)\right] \tag{A5}$$

APPENDIX B: DERIVATION OF THE AMPLITUDE F IN THE MOMENTUM SPACE

In this appendix, we show explicitly how to derive Eq. (30) from Eq. (28). First, we perform the Fourier transformation on the hard scattering kernel $\tilde{T}_{\beta\alpha}(z)$ and obtain

$$F = \int \mathrm{d}^4z\tilde{\Phi}_{\alpha\beta}(z)\int\frac{\mathrm{d}^4l}{(2\pi)^4}e^{il\cdot z}T_{\beta\alpha}(l) = \int\frac{\mathrm{d}^4l}{(2\pi)^4}\left[\int\mathrm{d}^4ze^{il\cdot z}\tilde{\Phi}_{\alpha\beta}(z)\right]T_{\beta\alpha}(l) \tag{B1}$$

Performing Fourier transformation to the matrix element $\tilde{\Phi}_{\alpha\beta}(z)$ in Eq. (27), and using $z^\mu e^{il\cdot z} = -i\frac{\partial}{\partial l_\mu}e^{il\cdot z}$, we can obtain

$$\int \mathrm{d}^4ze^{il\cdot z}\tilde{\Phi}_{\alpha\beta}(z) = \frac{-if_B}{4}\int\mathrm{d}^4z\left\{\left[m_B\tilde{\phi}_P + \frac{-i}{2}\tilde{\phi}_T\left(P^\mu\frac{\partial}{\partial l_\nu} - P^\nu\frac{\partial}{\partial l_\mu}\right)\sigma_{\mu\nu} + \left(\tilde{\phi}_{A1}P^\mu + m_B\tilde{\phi}_{A2}\frac{\partial}{\partial l_\mu}\right)\gamma_\mu\right]e^{il\cdot z}\cdot\gamma^5\right\}_{\alpha\beta} \tag{B2}$$

Substituting Eq. (B2) into Eq. (B1), and making use of partial integration, the derivative $\frac{\partial}{\partial l_\mu}$ can be moved to act on the hard scattering kernel $T_{\beta\alpha}(l)$. In addition, we observe that in the four distribution amplitudes in Eq. (23) and Eqs. (26a)–(26b), only the exponential part $e^{-ik_q\cdot z}$ depends on the variable z. Therefore the integration over z can be easily worked out and the result is a delta function $(2\pi)^4\delta^{(4)}(l-k_q)$.

$$F = \int\frac{\mathrm{d}^4l}{(2\pi)^4}(2\pi)^4\delta^{(4)}(l-k_q)[\ldots]T_{\beta\alpha}(l) \tag{B3}$$

After taking $P^\mu = m_Bv^\mu$ and $k_q^2 = m_q^2$ [Eq. (11b)] into consideration, we obtain the final expression in Eq. (30).

APPENDIX C: EXPLICIT EXPRESSIONS OF EQ. (44) AND $Z_2^{b,\bar{u}}$

We use the dimensional regularization for the ultraviolet divergence and introduce a small mass λ for gluons to regularize the infrared divergence in Eq. (44). The naive dimensional regularization is adopted, where γ^5 anticommutes with all other gamma matrices.

The conventions and notations we use are

$$\alpha_s = \frac{g_s^2}{4\pi}\quad C_F = \frac{N^2-1}{2N}\quad \sigma^{\mu\nu} = \frac{i}{2}[\gamma^\mu,\gamma^\nu],$$
$$\mathrm{P}_L = \frac{1-\gamma^5}{2}\quad \mathrm{P}_R = \frac{1+\gamma^5}{2}\quad \gamma_L^\mu = \gamma^\mu\mathrm{P}_L\quad \gamma_R^\mu = \gamma^\mu\mathrm{P}_R.$$

With the help of the program *Package-X* [73,74], the explicit result of Eq. (44) is

$$F_V^{(1)\mu} = \frac{1}{(2\pi)^3}\sqrt{\frac{m_um_b}{k^0(p-k)^0}}\frac{\alpha_sC_F}{4\pi}\bar{v}^r(k)\cdot\mathbf{INT}\cdot u^s(p-k) \tag{C1}$$

where

$$\begin{aligned}\mathbf{INT} = {}& \gamma_L^\mu\cdot\left[\frac{1}{\varepsilon}-\gamma_\mathrm{E}+\ln\frac{4\pi\mu^2}{m_um_b}+x\ln\frac{x+1}{x-1}\ln\frac{\lambda^2}{m_um_b}+F(x,x_1,x_2)\right]+\gamma_R^\mu\cdot\frac{\sqrt{x^2-1}}{2}\ln\frac{x+1}{x-1}\\ &+\frac{i}{2}\sigma^{\mu\nu}\mathrm{P}_L\frac{p_\nu}{m_u}\frac{x-x_2}{x_1-x_2}\left[\ln\frac{x+x_1}{x-x_2}-x_1\ln\frac{x+1}{x-1}\right]+\frac{i}{2}\sigma^{\mu\nu}\mathrm{P}_R\frac{p_\nu}{m_b}\frac{x+x_1}{x_1-x_2}\left[x_2\ln\frac{x+1}{x-1}-\ln\frac{x+x_1}{x-x_2}\right]\\ &+\mathrm{P}_L\frac{p^\mu}{m_u}\frac{x-x_2}{x_1-x_2}\left[-2+\left(\frac{3}{2}+\frac{x_1+x_2}{x_1-x_2}\right)\ln\frac{x+x_1}{x-x_2}+\left(\frac{2}{x_1-x_2}+x+\frac{3}{2}x_1\right)\ln\frac{x+1}{x-1}\right]\\ &+\mathrm{P}_R\frac{p^\mu}{m_b}\frac{x+x_1}{x_1-x_2}\left[2+\left(\frac{3}{2}-\frac{x_1+x_2}{x_1-x_2}\right)\ln\frac{x+x_1}{x-x_2}+\left(\frac{2}{x_1-x_2}+x-\frac{3}{2}x_2\right)\ln\frac{x+1}{x-1}\right]\end{aligned} \tag{C2}$$

and the finite part $F(x,x_1,x_2)$ is

$$\begin{aligned}F(x,x_1,x_2) = {}& \frac{x}{2}\left[\left(3-2\ln\frac{\sqrt{(x_1^2-1)(x_2^2-1)}}{x^2-1}\right)\ln\frac{x+1}{x-1}-\left(\ln\frac{x_1+1}{x+x_1}\right)^2-\left(\ln\frac{x_2+1}{x_1-x_2}\right)^2+\left(\ln\frac{x_1+1}{x_1-x_2}\right)^2+\left(\ln\frac{x_2+1}{x_1-x_2}\right)^2\right.\\ &\left.-2\ln\frac{x_1+1}{x+x_1}\ln\frac{x_1+1}{x_1-x_2}+2\ln\frac{x_2+1}{x_1-x_2}\ln\frac{x_2+1}{x-x_2}+4\ln\frac{x_1-1}{x_2-1}\ln\frac{2}{x_1-x_2}+4\left(\mathrm{Li}_2\frac{1-x_1}{2}-\mathrm{Li}_2\frac{1-x_2}{2}\right)\right]\end{aligned} \tag{C3}$$

In Eqs. (C2) and (C3), γ_E is the Euler-Mascheroni constant, $\mathrm{Li}_2(z)$ is the polylogarithm function of order 2, and the definitions of x, x_1, x_2 are

$$x = \frac{m_b^2 + m_u^2 - p^2}{\sqrt{\kappa(m_b^2, m_u^2, p^2)}}$$
$$x_1 = \frac{m_b^2 - m_u^2 + p^2}{\sqrt{\kappa(m_b^2, m_u^2, p^2)}}$$
$$x_2 = \frac{m_b^2 - m_u^2 - p^2}{\sqrt{\kappa(m_b^2, m_u^2, p^2)}}$$

where $\kappa(m_b^2, m_u^2, p^2)$ is the Källén function or triangle function

$$\kappa(m_b^2, m_u^2, p^2) = (m_b^2)^2 + (m_u^2)^2 + (p^2)^2 - 2m_b^2 p^2 - 2m_u^2 p^2 - 2m_b^2 m_u^2.$$

The renormalization constant $Z_2^{b,\bar{u}}$ in Eq. (46) has been computed in the virtial gluon-mass regularization scheme and with the on-shell renormalization condition. The result is

$$Z_2^{b,\bar{u}} = 1 + \frac{\alpha_s C_F}{4\pi}\left(-\frac{1}{\varepsilon} + \gamma_E - \ln\frac{4\pi\mu^2}{m_{b,\bar{u}}^2} - 4 - 2\ln\frac{\lambda^2}{m_{b,\bar{u}}^2}\right). \tag{C4}$$

[1] M. Beneke, G. Buchalla, M. Neubert, and C. T. Sachrajda, Phys. Rev. Lett. **83**, 1914 (1999).
[2] M. Beneke, G. Buchalla, M. Neubert, and C. T. Sachrajda, Nucl. Phys. **B591**, 313 (2000).
[3] M. Beneke, G. Buchalla, M. Neubert, and C. T. Sachrajda, Nucl. Phys. **B606**, 245 (2001).
[4] M. Beneke and M. Neubert, Nucl. Phys. **B675**, 333 (2003).
[5] Y.-Y. Keum, H.-n. Li, and A. I. Sanda, Phys. Lett. B **504**, 6 (2001).
[6] Y. Y. Keum, H.-N. Li, and A. I. Sanda, Phys. Rev. D **63**, 054008 (2001).
[7] C.-D. Lu, K. Ukai, and M.-Z. Yang, Phys. Rev. D **63**, 074009 (2001).
[8] Y.-Y. Keum, H.-n. Li, and A. I. Sanda, Proceedings, 9th International Symposium on Heavy Flavor Physics, *AIP Conf. Proc.* 618, 229 (2002).
[9] Y.-Y. Keum, T. Kurimoto, H. N. Li, C.-D. Lu, and A. I. Sanda, Phys. Rev. D **69**, 094018 (2004).
[10] A. G. Grozin and M. Neubert, Phys. Rev. D **55**, 272 (1997).
[11] M. Beneke and T. Feldmann, Nucl. Phys. **B592**, 3 (2001).
[12] B. O. Lange and M. Neubert, Phys. Rev. Lett. **91**, 102001 (2003).
[13] S. J. Lee and M. Neubert, Phys. Rev. D **72**, 094028 (2005).
[14] H. Kawamura, J. Kodaira, C.-F. Qiao, and K. Tanaka, Phys. Lett. B **523**, 111 (2001); **536**,344(E) (2002).
[15] T. Huang, X.-G. Wu, and M.-Z. Zhou, Phys. Lett. B **611**, 260 (2005).
[16] T. Huang, C.-F. Qiao, and X.-G. Wu, Phys. Rev. D **73**, 074004 (2006).
[17] C.-W. Hwang, Phys. Rev. D **81**, 114024 (2010).
[18] G. Bell, T. Feldmann, Y.-M.Wang, and M. W. Y. Yip, J. High Energy Phys. 11 (2013) 191.
[19] H. Leutwyler and M. Roos, Z. Phys. C **25**, 91 (1984).
[20] M.-Z. Yang, Eur. Phys. J. C **72**, 1880 (2012).
[21] J.-B. Liu and M.-Z. Yang, J. High Energy Phys. 07 (2014) 106.
[22] J.-B. Liu and M.-Z. Yang, Phys. Rev. D **91**, 094004 (2015).
[23] A. A. Penin and M. Steinhauser, Phys. Rev. D **65**, 054006 (2002).
[24] J. Bordes, J. Penarrocha, and K. Schilcher, J. High Energy Phys. 12 (2004) 064.
[25] J. Bordes, J. Penarrocha, and K. Schilcher, J. High Energy Phys. 11 (2005) 014.
[26] W. Lucha, D. Melikhov, and S. Simula, Phys. Lett. B **701**, 82 (2011).
[27] S. Narison, Phys. Lett. B **718**, 1321 (2013).
[28] P. Gelhausen, A. Khodjamirian, A. A. Pivovarov, and D. Rosenthal, Phys. Rev. D **88**, 014015 (2013); **91**, 099901(E) (2015).
[29] S. Narison, Nucl. Part. Phys. Proc. **270–272**, 143 (2016).
[30] Z.-G. Wang, W.-M. Yang, and S.-L. Wan, Nucl. Phys. **A744**, 156 (2004).
[31] G. Cvetič, C. S. Kim, G.-L.Wang, and W. Namgung, Phys. Lett. B **596**, 84 (2004).
[32] A. M. Badalian, B. L. G. Bakker, and Yu. A. Simonov, Phys. Rev. D **75**, 116001 (2007).
[33] T. Branz, T. Gutsche, V. E. Lyubovitskij, I. Schmidt, and A. Vega, Phys. Rev. D **82**, 074022 (2010).
[34] S. Godfrey and N. Isgur, Phys. Rev. D **32**, 189 (1985).
[35] P. Colangelo, G. Nardulli, and M. Pietroni, Phys. Rev. D **43**, 3002 (1991).
[36] M. Di Pierro and E. Eichten, Phys. Rev. D **64**, 114004 (2001).
[37] D. Ebert, R. N. Faustov, and V. O. Galkin, Phys. Lett. B **635**, 93 (2006).
[38] C. T. H. Davies *et al.* (Fermilab Lattice, HPQCD, UKQCD, MILC Collaboration), Phys. Rev. Lett. **92**, 022001 (2004).
[39] A. Gray, M. Wingate, C. T. H. Davies, E. Dalgic, G. P. Lepage, Q. Mason, M. Nobes, and J. Shigemitsu (HPQCD), Phys. Rev. Lett. **95**, 212001 (2005).
[40] C. T. H. Davies, C. McNeile, E. Follana, G. P. Lepage, H. Na, and J. Shigemitsu, Phys. Rev. D **82**, 114504 (2010).
[41] C. McNeile, C. T. H. Davies, E. Follana, K. Hornbostel, and G. P. Lepage, Phys. Rev. D **85**, 031503 (2012).

[42] A. Bazavov *et al.* (Fermilab Lattice, MILC Collaboration), Phys. Rev. D **85**, 114506 (2012).
[43] D. Becirevic, V. Lubicz, F. Sanfilippo, S. Simula, and C. Tarantino, J. High Energy Phys. 02 (2012) 042.
[44] H. Na, C. J. Monahan, C. T. H. Davies, R. Horgan, G. P. Lepage, and J. Shigemitsu, Phys. Rev. D **86**, 034506 (2012).
[45] R. J. Dowdall, C. T. H. Davies, R. R. Horgan, C. J. Monahan, and J. Shigemitsu (HPQCD), Phys. Rev. Lett. **110**, 222003 (2013).
[46] K. A. Olive *et al.* (Particle Data Group Collaboration), Chin. Phys. C **38**, 090001 (2014).
[47] I. Adachi *et al.* (Belle Collaboration), Phys. Rev. Lett. **110**, 131801 (2013).
[48] B. Kronenbitter *et al.* (Belle Collaboration), Phys. Rev. D **92**, 051102 (2015).
[49] J. P. Lees *et al.* (*BABAR* Collaboration), Phys. Rev. D **88**, 031102 (2013).
[50] B. Aubert *et al.* (*BABAR* Collaboration), Phys. Rev. D **81**, 051101 (2010).
[51] J. L. Rosner, S. Stone, and R. S. Van de Water, arXiv: 1509.02220.
[52] M. Barrett (Belle II Collaboration), Proceedings, 13th Conference on Flavor Physics and CP Violation (FPCP 2015), *Proc. Sci.*, FPCP2015 (2015) 049.
[53] B. Wang (Belle-II Collaboration), J. Univ. Sci. Tech. China **46**, 617 (2016).
[54] M. Wirbel, B. Stech, and M. Bauer, Z. Phys. C **29**, 637 (1985).
[55] E. Eichten, K. Gottfried, T. Kinoshita, K. D. Lane, and T.-M. Yan, Phys. Rev. D **17**, 3090 (1978); **21**, 313(E) (1980).
[56] E. Eichten, K. Gottfried, T. Kinoshita, K. D. Lane, and T.-M. Yan, Phys. Rev. D **21**, 203 (1980).
[57] A. De Rujula, H. Georgi, and S. L. Glashow, Phys. Rev. D **12**, 3589 (1975).
[58] G. Altarelli, N. Cabibbo, G. Corbo, L. Maiani, and G. Martinelli, Nucl. Phys. **B208**, 365 (1982).
[59] P. Colangelo, F. De Fazio, M. Ladisa, G. Nardulli, P. Santorelli, and A. Tricarico, Eur. Phys. J. C **8**, 81 (1999).
[60] C.-W. Hwang, Phys. Rev. D **81**, 054022 (2010).
[61] N. Carrasco *et al.*, Proceedings, 31st International Symposium on Lattice Field Theory (Lattice 2013), *Proc. Sci.*, LATTICE2013 (2014) 313 [arXiv:1311.2837].
[62] Y. Aoki, T. Ishikawa, T. Izubuchi, C. Lehner, and A. Soni, Phys. Rev. D **91**, 114505 (2015).
[63] N. H. Christ, J. M. Flynn, T. Izubuchi, T. Kawanai, C. Lehner, A. Soni, R. S. Van de Water, and O. Witzel, Phys. Rev. D **91**, 054502 (2015).
[64] Z.-G. Wang, Eur. Phys. J. C **75**, 427 (2015).
[65] P. Pakhlov and T. Uglov, J. Phys. Conf. Ser. **675**, 022009 (2016).
[66] Z.-T. Wei and M.-Z. Yang, Nucl. Phys. **B642**, 263 (2002).
[67] A. G. Grozin, Int. J. Mod. Phys. A **20**, 7451 (2005).
[68] G. Bell and T. Feldmann, J. High Energy Phys. 04 (2008) 061.
[69] T. Feldmann, B. O. Lange, and Y.-M.Wang, Phys. Rev. D **89**, 114001 (2014).
[70] P. Ball, J. High Energy Phys. 01 (1999) 010.
[71] S. Descotes-Genon and C. T. Sachrajda, Nucl. Phys. **B650**, 356 (2003).
[72] T. H. Boyer, Ann. Phys. (N.Y.) **44**, 1 (1967).
[73] H. H. Patel, Comput. Phys. Commun. **197**, 276 (2015).
[74] H. H. Patel, arXiv:1612.00009.